Orbital Debris Radar Measurements from the Haystack Ultra-wideband Satellite Imaging Radar (HUSIR): 2014-2017

James Murray[(1)], Rossina Miller[(1)], Mark Matney[(2)], and Timothy Kennedy[(2)]

[(1)] Jacobs, NASA Johnson Space Center, Mail Code XI5-9E, 2101 NASA Parkway, Houston, TX 77058, USA, james.i.murray@nasa.gov

[(2)] NASA Johnson Space Center, Mail Code XI5-9E, 2101 NASA Parkway, Houston, TX 77058, USA

ABSTRACT

For many years, the NASA Orbital Debris Program Office (ODPO) has partnered with the U.S. Department of Defense and the Massachusetts Institute of Technology Lincoln Laboratory (MIT/LL) to collect data on the orbital debris environment using the Haystack radar. These measurements are used to characterize the small debris environment in low Earth orbit (LEO), down to a noise-limited size of approximately 5 mm—depending on altitude. The Haystack radar operated by MIT Lincoln Lab underwent upgrades starting in May 2010, with operations resuming in 2014 as the Haystack Ultra-wideband Satellite Imaging Radar (HUSIR). Hence, the data collected beginning in 2014 represents the first dataset available from this upgraded sensor. HUSIR is the primary source of data used by the ODPO to statistically sample orbital debris in the 5-mm to 10-cm size regime in LEO and is a key source of data to build and validate the NASA Orbital Debris Engineering Model. In this paper, we will present recent results from measurements performed during the US Government fiscal years 2014 – 2017. Using the NASA Size Estimation Model, a method based on laboratory radar measurements of debris, we will compare the size distributions of selected orbital debris populations over this 4-year period and flux measurements of orbital debris greater than 1 cm.

1 INTRODUCTION

The NASA Orbital Debris Program Office (ODPO) relies primarily on ground-based radar measurements to characterize the distribution of small debris in low Earth orbit (LEO). The Massachusetts Institute of Technology Lincoln Laboratory (MIT/LL) has collected radar measurements for the NASA ODPO for nearly three decades under memorandums of agreement with the U.S. Department of Defense. Beginning with the Haystack radar in October 1990 and supplemented by the Haystack Auxiliary Radar (HAX) radar in March 1994, the NASA ODPO nominally receives 1000 hours of data collected per fiscal year (FY). The Haystack radar operated by MIT/LL underwent upgrades starting in May 2010, with operations resuming in 2014 as the Haystack Ultra-wideband Satellite Imaging Radar (HUSIR). Hence, the data collected beginning in 2014 represents the first dataset available from this upgraded sensor.

Due to the sensitivity of these radars, NASA ODPO is able to sample the orbital debris environment down to approximately 3 cm with HAX and 5 mm with HUSIR to an altitude of up to 1000 km. NASA ODPO uses data collected by HUSIR and HAX to characterize the orbital debris environment in altitude, inclination, and size for a large fraction of LEO (altitude < 2000 km) and orbits traversing LEO.

In this paper, we will present recent results from measurements performed during the years FY2014 – FY2017 with HUSIR. Using the NASA Size Estimation Model, a method based on laboratory radar measurements of debris, we will compare the size distributions of selected orbital debris populations over this 4-year period and flux measurements of orbital debris greater than 1 cm.

An in depth discussion of the NASA ODPO radar data collection, signal processing, and data analysis on data delivered from MIT/LL is available in [1].

2 DATA COLLECTION OVERVIEW

As mentioned in section 1, the dataset presented in this paper was collected from FY2014 to FY2017 using the HUSIR radar after the Haystack radar underwent a significant upgrade to incorporate a W-band transmitter and

receiver. The upgrade also included a new radome, quadrupod, backstructure, and azimuth bearings. Additional in-depth information regarding the upgrade may be found in [2].

Both the HUSIR and HAX radars are located in Tyngsborough, Massachusetts with a Cassegrain focus at the locations found in Table 1 with respect to the 1984 World Geodetic System (WGS 84) Earth model [1].

Table 1. HUSIR and HAX Location with Respect to the 1984 World Geodetic System (WGS 84) Earth Model

	Latitude	Longitude	Elevation
HUSIR	42.623287° N	288.511846° E	115.69 m
HAX	42.622835° N	288.511709° E	101.11 m

The sensitivity of HUSIR can be calculated as the single pulse signal-to-noise ratio (SNR) measured on an object with a 1-square meter-radar cross section (RCS) at 1000 km range. Using the nominal HUSIR operating parameters, this yields a sensitivity of 59.2 dB. The actual sensitivity can vary, mostly due to variations in transmission power, which must be taken into account when comparing the datasets across years. In particular, FY2017 had drastically reduced sensitivity as compared to previous years, as can be seen in Fig. 1.

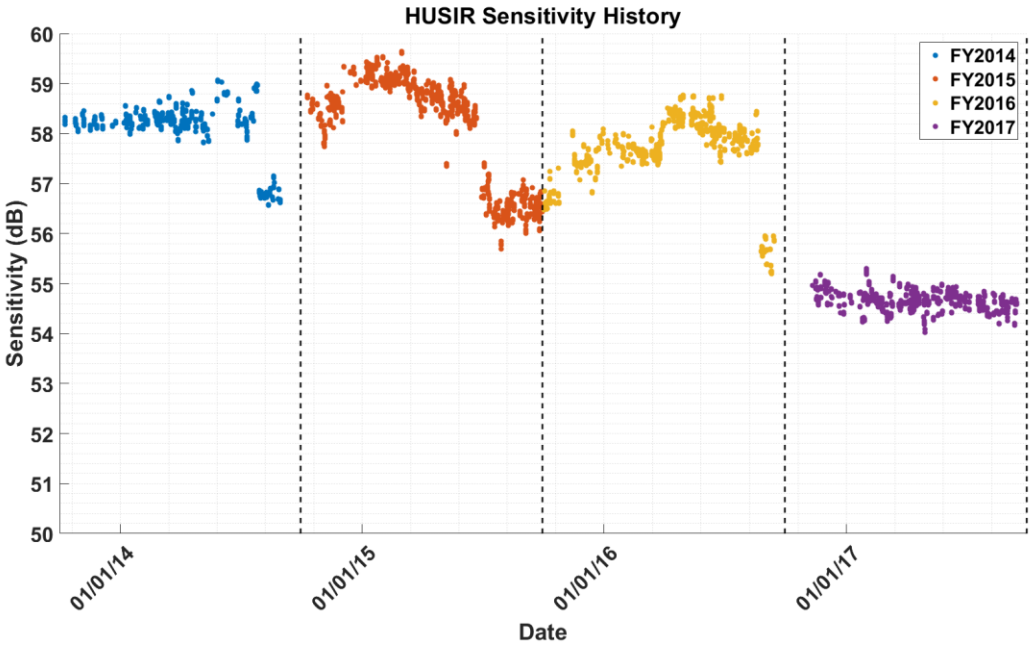

Fig. 1. Sensitivity history for HUSIR from the beginning of FY2014 through the end of FY2017.

For orbital debris radar data collection the HUSIR radar operates in a "beam-park" mode in which the radar antenna is pointed at a fixed elevation and azimuth, allowing the debris environment to randomly pass through the radar beam. This provides a fixed detection volume that simplifies calculations of the debris flux, or number of objects detected per unit area, per unit time. The tradeoff of the beam-park mode is that it limits precise measurement of a given object's orbital parameters, due to the short observation time for each object.

The data presented here was taken staring at an azimuth of 90° and an elevation of 75°, referred to as 75E. By staring just off-zenith, the 75E staring geometry allows the radar to measure Doppler shifts that give meaningful orbital information for orbital inclinations between approximately 40° inclination and 140° inclination – assuming a circular orbit. The high-elevation angle of the 75E staring geometry also minimizes atmospheric attenuation, allowing the radar to detect very small debris objects in orbit. Additional data from these radars were collected at other orientations for specific campaigns, including low elevation staring south to observe lower inclination orbits, but results from those campaigns are not included in this paper.

Table 2 presents a summary of the number of observation hours contained in the dataset and the number of detections observed. The number of detections represents the total number of events for which there were three or more pulses with an integrated SNR greater than 5.65 dB, where at least one is in the two-way, 6 dB beamwidth (one-way, two-sided 3 dB-beamwidth).

Table 2. Data Collection Summary

Fiscal Year	Hours of Observation	Number of Detections
2014	268.1	4107
2015	288.4	4858
2016	458.5	7079
2017	496.2	5701

2.1 The NASA Size Estimation Model

The NASA SEM was developed to relate RCS to the physical size of an on-orbit debris fragment [3]. The characteristic length of an object is defined as the average of the largest dimensions for an object measured along three orthogonal axes. The first axis was chosen to coincide with the largest dimension, the second axis to coincide with the largest dimension in a plane orthogonal to the first axis, and the third axis to be orthogonal to the plane defined by the first two axes. The characteristic length of an object is referred to interchangeably as size or diameter.

In Fig. 2 the results of RCS-to-size measurements on 39 representative debris objects are shown, where each point represents an average RCS over many orientations for a single object measured at a single frequency. The oscillating curve is the RCS for a spherical conductor while the smooth curve is the polynomial fit to the data and comprises the NASA SEM.

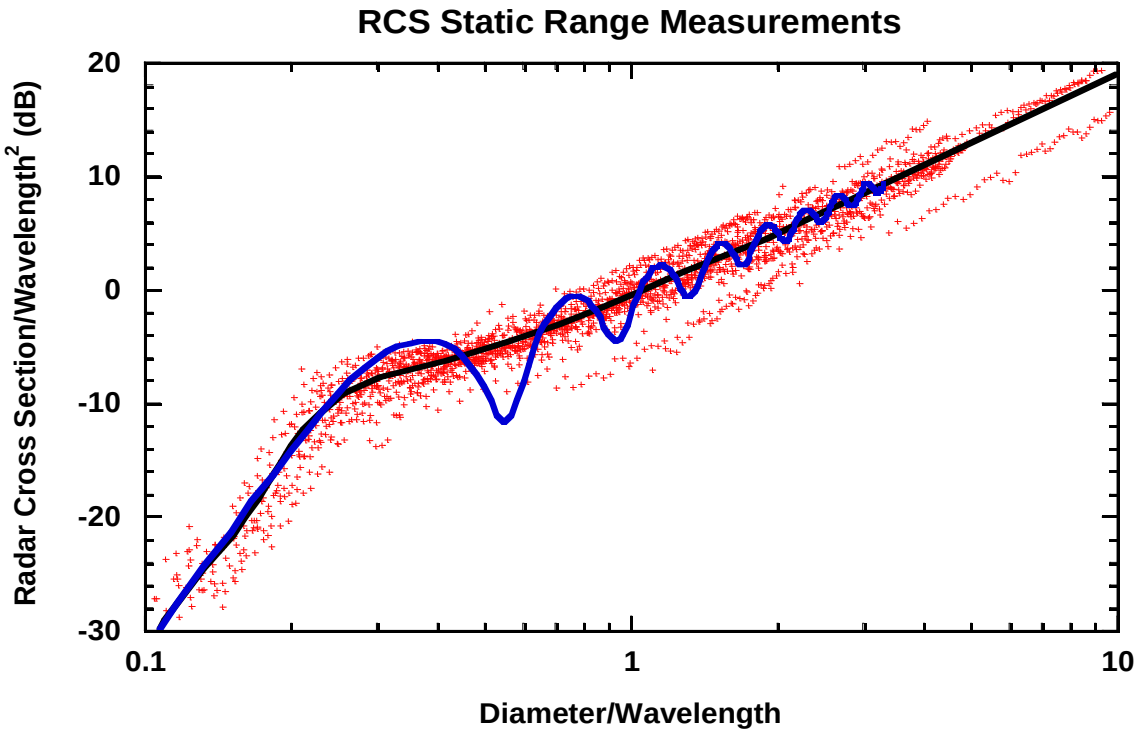

Fig. 2. Results of RCS-to-size measurements on 39 representative debris objects. The oscillating line is the RCS for a spherical conductor while the smooth line is the polynomial fit to the data.

3 ENVIRONMENT OVERVIEW

The radar data presented here is meant to provide a broad overview of the state of the debris environment in low Earth orbit. Since the radar sensitivity changes from year to year, flux charts presented in this section, which compare all years of data, are presented with the flux integrated down to a limiting size.

3.1 Surface Area Flux versus Altitude

Flux is defined as the number of detections through the lateral surface area of the radar beam within a given period. Total flux represents the flux of all objects regardless of size, where size is estimated using the NASA SEM, as described in section 2.1. To aid in comparing different years, cumulative flux to a limiting size is shown. This represents the flux of objects with a size equal to or greater than the chosen limiting size. For all years, cumulative flux is presented to limiting sizes of 5.5 mm and 1 cm, depending upon altitude. To avoid presenting potentially misleading information, each flux chart is limited to altitudes where it is estimated that radars are sensitive to objects of a specific size and above, which is referred to as complete. This corresponds to approximately 1000 km for a limiting size of 5.5 mm and 1600 km for a limiting size of 1 cm. All flux versus altitude charts are presented using 50 km-altitude bins.

Fig. 3 shows the cumulative flux versus altitude limited to 5.5 mm for all 75° elevation data, by year. For FY2014 - FY2016, the flux distributions appear stable. The FY2017 flux of objects 5.5 mm and larger appears to diverge from earlier years at around 850 km. This divergence may be attributed to the reduced sensitivity in FY2017, which resulted in a lower "completeness" altitude, and reduced detections for higher altitudes.

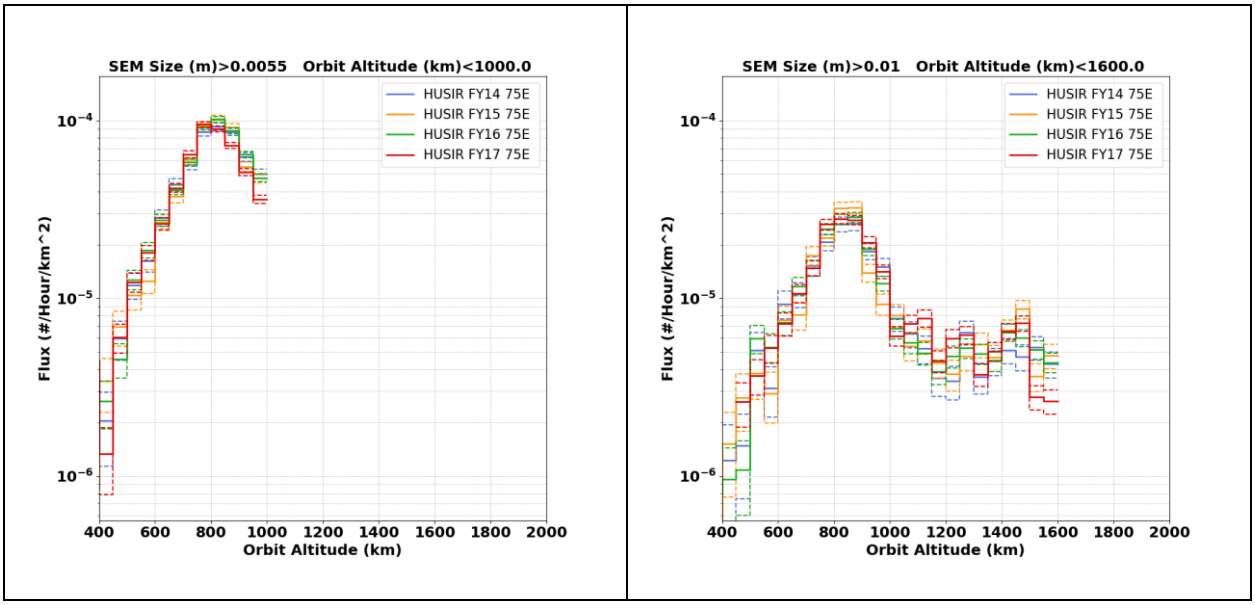

Fig. 3. Cumulative surface area flux versus altitude limited to 1 cm and 5.5 mm, by year. The dashed lines represent Poisson 1σ uncertainty bounds

3.2 Surface Area Flux versus Inclination

In addition to flux versus altitude, examining flux versus inclination gives more insight to the distinct populations/families of debris. Flux is defined in the same fashion as above, except that the beam area is the total surface area of the beam from the minimum observable altitude to the maximum observable altitude, since each altitude bin can measure debris at all inclinations available to the radar in the 75° east-staring geometry. The fluxes presented in this section will be to limiting sizes of 5.5 mm and 1 cm and use 2° sized bins.

When flux is broken down by inclination, very distinct groupings become apparent, as shown in Fig. 4. The most prominent are those between 94° and 105° associated with the sun-synchronous family of orbits, 71° and 78°, which is associated with Cosmos 2251 of the Iridium 33-Cosmos 2251 collision; and 63° and 67°, which is associated with the NaK coolant droplets ejected from RORSAT nuclear reactors. Additionally, an uncorrelated family of debris in the 81° to 87° inclination band has been identified and is currently under investigation to determine the source.

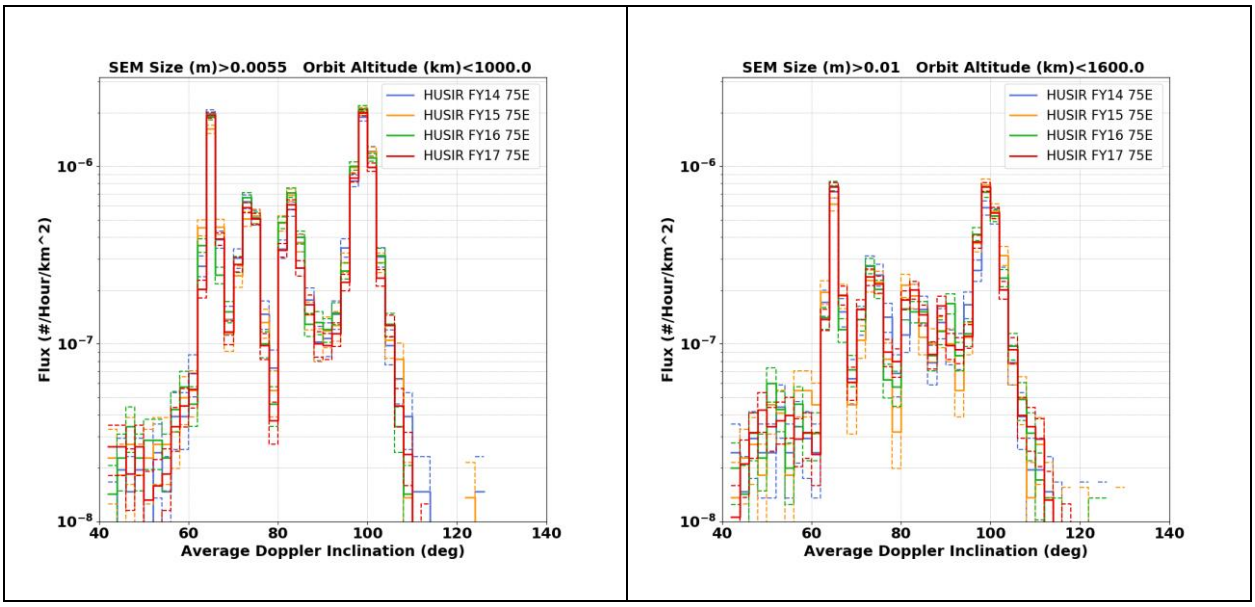

Fig. 4. Cumulative surface area flux versus inclination limited to 1 cm and 5.5 mm by year. The dashed lines represent 1σ uncertainty bounds.

3.3 SEM-size Cumulative Distribution

The total count rate of debris changes from year to year due to fluctuations in radar sensitivity. Although the flux charts from previous sections circumvent this issue by examining flux to limiting sizes, looking at the cumulative size distributions provides insight into the behavior across a greater range of sizes. As seen in Fig. 5, for sizes down to approximately 6 mm, the size distributions each year are remarkably consistent. If one examines the behaviors at smaller sizes, it can be seen that the FY2017 distribution rolls off more quickly than in other years, which is consistent with the reduced sensitivity in FY2017. FY2017 also appears to differ from other years for objects greater than approximately 20 cm. The reason for this is currently not known. An estimate of the Poisson uncertainty in the count rate is shown using dashed lines to represent the estimated 1-sigma (σ) confidence intervals.

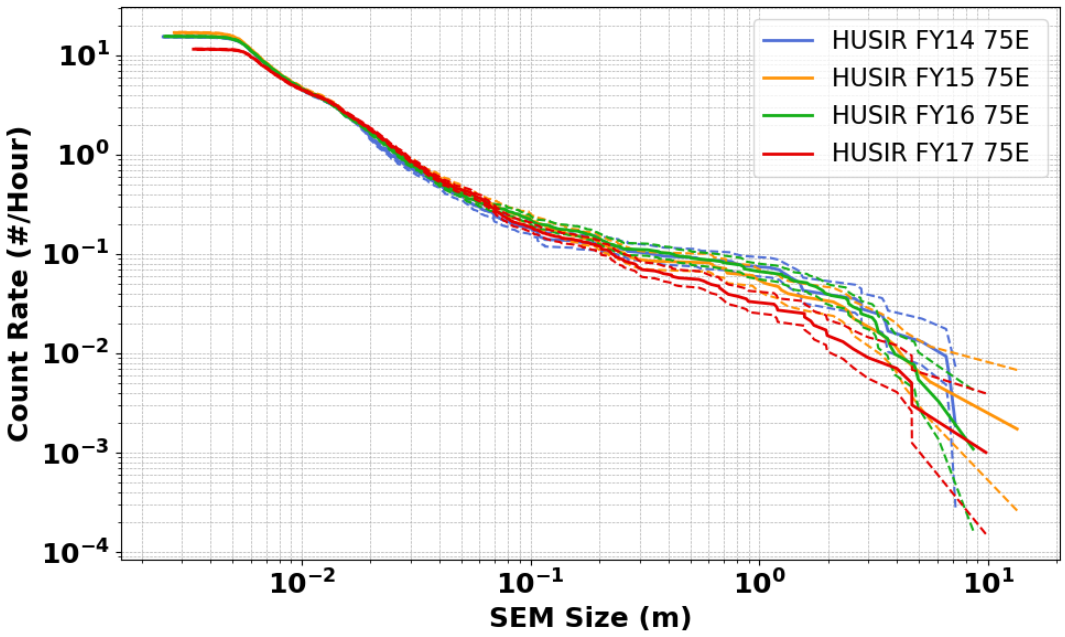

Fig. 5. SEM-size Cumulative Distribution by year.

4 ENVIRONMENT EVOLUTION

4.1 Significant Debris Events in Space

Between the beginning of FY2014 and the end of FY2017, 19 breakup events and 10 anomalous events were observed [4]. Breakup events are characterized by the energetic separation of fragments from the parent body. Anomalous events are characterized by low-energy fragment separation like the shedding of multi-layer insulation blankets or separation of a single object. Due to the energetic nature of breakup events, the number of debris objects created during the event typically is significantly greater than the number of debris objects created by an anomalous event.

Of the 19 breakup events, 2 events were significant enough to earn a place in the top 10 largest debris clouds on orbit. USA 109 exploded due to a battery failure on 3 February 2015 that resulted in an initial 236 cataloged debris objects, 219 of which are still on-orbit as of 4 July 2019, giving it the distinction of the eighth largest debris cloud on-orbit. NOAA-16 fragmented due to an unknown cause on 25 November 2015, which resulted in 458 cataloged debris objects, all of which are still on-orbit as of 4 July 2019. This makes the NOAA-16 breakup the third largest on-orbit debris cloud, behind only the People's Republic of China (PRC) Anti-Satellite vehicle test against the PRC Fengyun-1C LEO weather spacecraft and the inadvertent collision of the derelict Russian Cosmos 2251 and active U.S. commercial Iridium 33 communication spacecraft.

Figure 6 shows the cumulative size distribution of debris detected between 850 km - 900 km altitude and 95°-105° inclinations for FY2014-FY2017, which roughly corresponds to the orbits of both major breakups during that time. The USA 109 breakup occurred in the second quarter of FY2015 and its effect is seen quite clearly as a large increase in debris detection rates of all sizes from FY2014 to FY2015. The NOAA-16 breakup occurred in the first quarter of FY2016 and can be seen in an increase of the number of detected debris objects greater than 3 cm. Finally, the FY2017 cumulative distribution shows signs of reduced count rates relative to FY2016, which may be indicative of debris generated by these events dragging out of the environment.

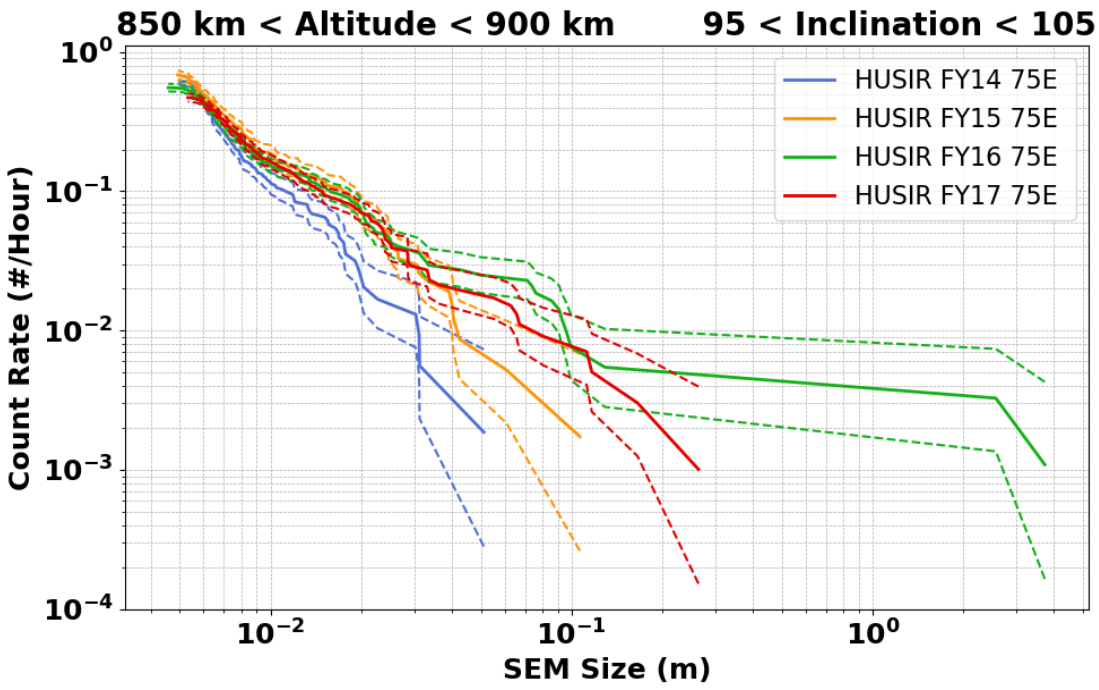

Fig. 6. Cumulative size distributions filtered in altitude and orbital inclination to illustrate the effects of the NOAA-16 and USA 109 breakups.

4.3 82° Inclination Debris Cloud

As discussed in section 3.2, this data set has revealed the existence of a new persistent cloud of debris in inclinations ranging from 81° to 87°, which has no accompanying large component, catalogued by the U.S. Space Surveillance Network. Figure 7 shows the cumulative size distribution of this 82° inclination debris cloud over 4 years. Not only does the cloud persist, the size distribution of the cloud remains stable from year to year. The major difference in the cumulative size distributions occurs for smaller sizes where each distribution begins to roll off at different sizes, which is related to the reduced sensitivity of HUSIR during that year. Further work is ongoing to better characterize this new debris cloud to the orbital debris environment.

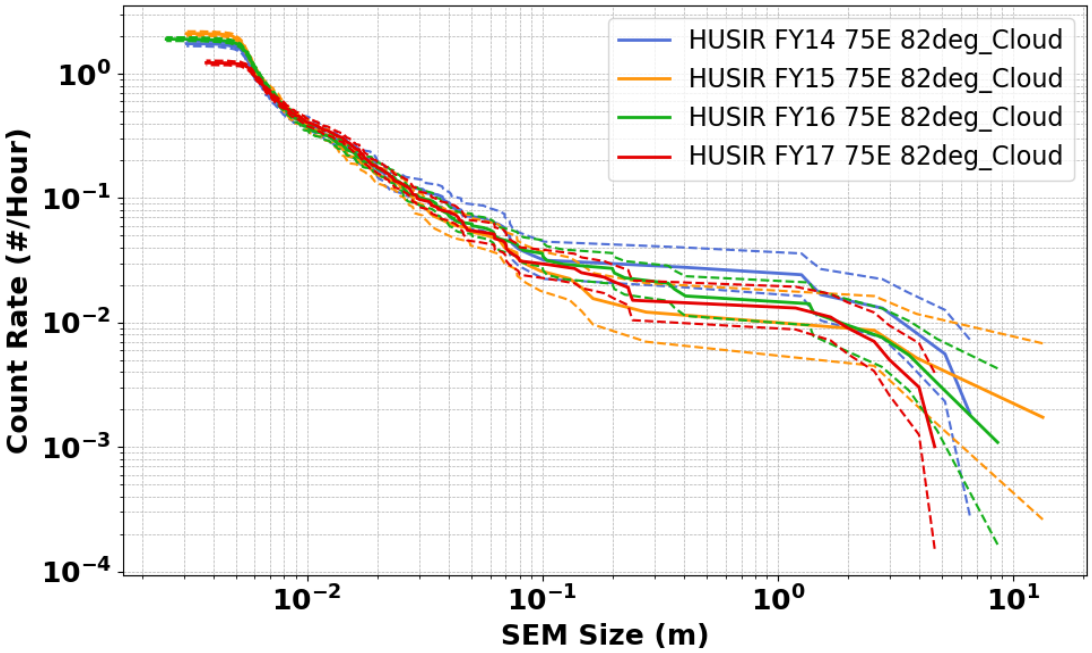

Fig. 7. Cumulative Size distribution of the 82° cloud.

5 SUMMARY

This paper presented measurements of the LEO orbital debris environment performed using the HUSIR radar. Although the NASA ODPO has partnered with the U.S. Department of Defense and the MIT/LL to collect data on the orbital debris environment using the Haystack radar for many years, the FY2014 – FY2017 data from HUSIR represents the first data set from this upgraded sensor. Detected objects in this dataset were measured for RCS, range, and range-rate. These data were analyzed to produce orbital altitude and inclination, size, and flux distributions.

During the time covered by this report, 19 breakup events and 10 anomalous events were observed. Of the 19 breakup events, 2 were large enough to earn spots in the list of 10 largest debris clouds on orbit. The effects of these breakup events on the debris environment and the evolution of the resultant clouds are readily apparent in the dataset. Additionally, a new cloud of debris in the 81° to 87° inclination band has been identified that has no accompanying known parent body, as catalogued by the U.S. Space Surveillance Network. The source of this new debris cloud is currently under investigation.

This paper presented a summary of the direct radar measurements that represent samples of the total debris population. The results presented here are a major source of information for updating LEO space debris environment models and predictions. To correctly apply these results, the NASA ODPO will carefully examine the capabilities and limitations of each radar and the sample populations observed.

6 REFERENCES

1. Murray, J., *et al*, "Haystack Ultra-Wideband Satellite Imaging Radar Measurements of the Orbital Debris Environment: 2014-2017," NASA/TP-2019-220302, 2019.
2. Czerwinski, M. G. and Usoff, J. M., "Development of the Haystack Ultrawideband Satellite Imaging Radar," MIT Lincoln Laboratory Journal, Volume 21, Number 1, pp. 28 – 44, 2014.
3. Lambour, R., *et al.*, Assessment of Orbital Debris Size Estimation from Radar Cross-Section Measurements, Adv. Space Res., v. 34, pp. 1013-1020, 2004.
4. Anz-Meador, P. D., *et al*, "History of On-Orbit Satellite Fragmentations 15th Edition," NASA/TM–2018–220037, 2018.